Technical Report No. 51

SACLANT ASW

RESEARCH CENTRE

DISTORTION OF BOTTOM REFLECTED PULSES

by

OLE. F. HASTRUP

1 MARCH 1966

NATO

VIALE SAN BARTOLOMEO, 92
LA SPEZIA, ITALY

This document is released to a NATO Government at the direction of the SACLANTCEN subject to the following conditions:

1. The recipient NATO Government agrees to use its best endeavours to ensure that the information herein disclosed, whether or not it bears a security classification, is not dealt with in any manner (a) contrary to the intent of the provisions of the Charter of the Centre, or (b) prejudicial to the rights of the owner thereof to obtain patent, copyright, or other like statutory protection therefor.

2. If the technical information was originally released to the Centre by a NATO Government subject to restrictions clearly marked on this document the recipient NATO Government agrees to use its best endeavours to abide by the terms of the restrictions so imposed by the releasing Government.

TECHNICAL REPORT NO. 51

SACLANT ASW RESEARCH CENTRE
Viale San Bartolomeo 92
La Spezia, Italy

DISTORTION OF BOTTOM REFLECTED PULSES

By

Ole F. Hastrup

1 March 1966

APPROVED FOR DISTRIBUTION

HENRIK NØDTVEDT

Director

[redacted]

Manuscript Completed:
18 August 1965

[redacted]

TABLE OF CONTENTS

DISTORTION OF BOTTOM REFLECTED PULSES

By

Ole F. Hastrup

ABSTRACT

The theory of linear systems combined with numerical Fourier transformations and inversion is used to obtain the shape of a general pressure pulse after its reflection from a general multilayered sea floor. The method is used to calculate the shape of the reflected shock and bubble pulses after reflection from models with up to three layers and for different angles of incidence.

INTRODUCTION

In the study of a sea bottom as a reflector it is of importance to be able to calculate the shape of the reflected pulse from the knowledge of the incident pulse, the elastic parameters of the bottom, and the layering system. Up to now the problem has been solved for special selected mathematical pulses reflected from a liquid half-space where only phase distortion is involved (Refs. 1, 2, 3 & 4), and not always with the same success.

It is, therefore, worth solving the problem in the general case where there is no limitation on the shape of the incident pulse nor on the number of solid layers in the bottom. This can be done by assuming plane waves and using numerical Fourier transformation and inversion, and by treating the bottom as a linear system.

1. THEORY

In the general case the reflection coefficient will be complex and frequency dependent, which means that a harmonic wave will be reflected not only with an amplitude change but also with a phase shift. Therefore, to handle the reflection of an arbitrary pulse f(t) we can expand this pulse into harmonic waves using a Fourier transformation given by:

$$F(\omega) = \int_{-\infty}^{\infty} f(t)\, e^{-i\omega t}\, dt$$

where ω is the angular frequency. $F(\omega)$ is generally complex. Denoting the complex reflection coefficient by $V(\omega)$, we know from the theory of linear systems (e.g. Ref. 5) that the output from $V(\omega)$ caused by a harmonic source is $V(\omega)e^{i\omega t}$, and from the formula for the inverse Fourier transformation we get the reflected pulse.

$$g(t) = \frac{1}{2\pi} \int_{-\infty}^{\infty} V(\omega) \cdot F(\omega)\, e^{i\omega t}\, d\omega$$

In the general case both $V(\omega)$ and f(t) are very complicated, and f(t) is often given graphically, which means that numerical methods have to be used for calculating g(t).

Because of the factor $e^{\pm i\omega t}$ in the integrals, it is impossible to use ordinary quadrature in evaluating these. We will, therefore, approximate the functions f(t) and $V(\omega) \cdot F(\omega)$ with a series of straight lines corresponding to a constant interval length.

Differentiating the approximating function twice, we obtain a sequence of impulses (Ref. 5):

$$f''(t) \approx \Sigma\ k_j \cdot \delta(t - t_j)$$

which, combined with

$$-\omega^2 F(\omega) = \int_{-\infty}^{\infty} f''(t)\ e^{-i\omega t}\ dt$$

gives

$$F(\omega) \approx -\frac{1}{\omega^2}\ \Sigma\ k_j \cdot e^{-i\omega t_j}$$

or, after some general calculations,

$$F(\omega) \simeq \frac{\sin^2\left(\frac{\omega \Delta t}{2}\right)}{\left(\frac{\omega \Delta t}{2}\right)^2}\ \Delta t\ \Sigma\ f(t_j)\ e^{-i\omega t_j} \qquad \text{(Eq. 1)}$$

Concerning the numerical inversion of $V(\omega) \cdot F(\omega) = G(\omega)$, because $g(t)$ is real, it can be expressed in the following way

$$g(t) = \frac{1}{\pi} \int_{-\infty}^{\infty} \left[a(\omega) \cos \omega t - b(\omega) \sin \omega t\right]\ d\omega$$

where

$$G(\omega) = a(\omega) + ib(\omega)$$

Again, by approximating $G(\omega)$ by a series of straight lines and differentiating twice, the inversion can be expressed, in the same way as Eq. 1, by

$$g(t) \simeq \frac{\sin^2\left(\frac{\Delta\omega t}{2}\right)}{\left(\frac{\Delta\omega t}{2}\right)^2} \cdot \frac{\Delta\omega}{\pi}\ \Sigma\ (a_j \cos \omega_j t - b_j \sin \omega_j t)$$

The determination of $V(\omega)$ is carried out using a matrix procedure suggested by W. T. Thompson (Ref. 6). To be able to handle the general case, damping has also been included in the method, as shown in Ref. 7.

2. NUMERICAL CALCULATIONS

To handle the above indicated equations, several programmes in ALGOL have been written for the Centre's Elliott 503 digital computer.

The calculation of the shape of the reflected pulse involves the use of two programmes, either

FOURIER INTEGRAL - PULSE SHAPE FROM PHASE SHIFT, or

FOURIER INTEGRAL - PULSE SHAPE FROM BOTTOM REFLECTIONS,

depending on whether it is a simple, liquid, one-layer bottom or the general, multi-layered bottom.

To check the method, the reflection of a sine pulse involving phase shift only has been used; when checked with the theoretical curves it was found to have an accuracy of the order of better than 2%. The results are shown in Fig. 1 for different angles of phase shift.

For visualising the pulses the Centre's Plotting table has been applied by using a plotter programme, thereby saving time in both plotting and drafting.

3. REFLECTION OF SHOCK AND BUBBLE PULSE

The signals chosen for investigation are the shock pulse and the first bubble pulse from the bombetta explosion of a 200 gm TNT charge. The combined shape is shown in Fig. 2, but, to facilitate the digitising, each pulse is handled separately because the time interval (20 ms) is great compared with the length of the pulse itself. Figures 3 and 4 show the spectra of the pulses. To cover the range from 0 - 12 kc sufficiently, steps of 25 cps were used. To simplify the calculations, time was scaled with one unit equal to 1 ms, which means that the frequency range was from 0 - 12.

(a) One-layered liquid bottom without damping

In this case the theory gives a reflection coefficient that is real and frequency-independent for angles of incidence less than the critical angle and is complex, with modulus equal one, after the critical angle. This means that in the first case there will be no distortion but only amplitude-reduction, and in the second there will be a phase-distortion depending on the angle of incidence and the bottom constants. Figure 5 gives the relation between angle of incidence, porosity, and phase shift.

The distortion of both the shock pulse and the bubble pulse has been calculated and the results are given on Figs. 6 and 7. Even if the two pulses had more or less the same shape before the reflection there is a very marked difference after, for example, a 60° phase shift does not change the shock pulse very much, whereas the bubble pulse almost looks inverted.

To be able to use the reflected pulse shape — in this case to calculate the phase shift and then also the porosity when the angle of incidence is known — the ratio between the maximum and minimum amplitude is plotted as a function of phase shift as shown in Fig. 8.

(b) Two and three-layered solid bottom

The data used for the models are the same as used in Ref. 7 and are given in Table 1. To give an idea about the reflection coefficient based on the two models, the reflection losses versus angle of incidence and frequency are given in Figs. 9-12.

TABLE 1

Model								
A	1	0	.5	0	0	1	-	Water
	1.055	0.26	0.468	1	1.5	1.89	1	45% porosity
	1.13	0.40	0.428	1.5	2.5	2.05	-	35% porosity
B	1	0	0.5	0	0	1	-	Water
	1.055	0.26	0.468	1	1.5	1.89	1	45% porosity
	1.133	0.40	0.428	1.5	2.5	2.05	1.5	35% porosity
	1.87	1.07	0.25	0.5	0.75	2.2	-	limestone

To check the accuracy in the time-scale first, the reflection from vertical incidence has been calculated using Models A and B, and A and B without damping, covering the time scale from −0.2 to 9.8 for both shock pulse and bubble pulse. The results are shown on Figs. 13 and 14. The calculated arrival times are given corresponding to the different reflections shown on the figures. To separate the rays, they are shown with a certain angle of incidence.

The calculated times correspond very closely to the curves, and the whole events of reflections from different layers show up very clearly.

The influence of angle of incidence is given for the different model configurations and pulses for the following angles: 0°, 20°, 40°, 60° and 80°. The results are shown on Figs. 15-22. In the case of model B the shape has been calculated for a longer time to show the reflections from the lowest interface.

To show the influence of the different models on the peak amplitudes, these are given in Figs. 23 and 24 as functions of the angle of incidence. The most obvious things one will observe are:

a) the very little difference between the two-layer and three-layer models in the case of the positive peaks,

b) the very little influence of shear for angles less than the critical, and

c) the considerably larger values for positive peaks in case of no shear.

Looking at the shape of the reflected pulse for 80° incidence it might be interesting to use Figs. 5 and 8 to calculate back to the porosity of the upper layer under the condition of no shear. The ratio $-\left(A/B\right)$ in Fig. 8 will be respectively 0.47 and 1.3 for shock and bubble pulses, which gives the angles 88° and 75° or, using the average 82° in Fig. 5, leads to a porosity of 43% compared with 45% used in the model.

REFERENCES

1. A.B. Arans and D.R. Yennie, Journ. Acoust. Soc. Am. 22, p. 231 (1950).

2. L.R.B. Duykers, "Deformation of a Specific Pulse Reflected beyond the Critical Angle", SACLANTCEN T.M. 28, June 1962, NATO UNCLASSIFIED.

3. W. Abramowitz, Journ. Acoust. Soc. Am. 36, p. 214 (L) (1964), and 37, p. 173 (L) (1965).

4. B.F. Cran and A.H. Nuttall, Journ. Acoust. Soc. Am. 37, p. 486 (1962).

5. A. Papaulis, "The Fourier Integral and its Applications", McGraw-Hill (1962).

6. W.T. Thompson, Journ. Appl. Phys., 21, p. 89 (1950).

7. O.F. Hastrup, "Reflection of Plane Waves From a Solid Multilayered Damping Bottom", SACLANTCEN T.R. No. 50, NATO UNCLASSIFIED.

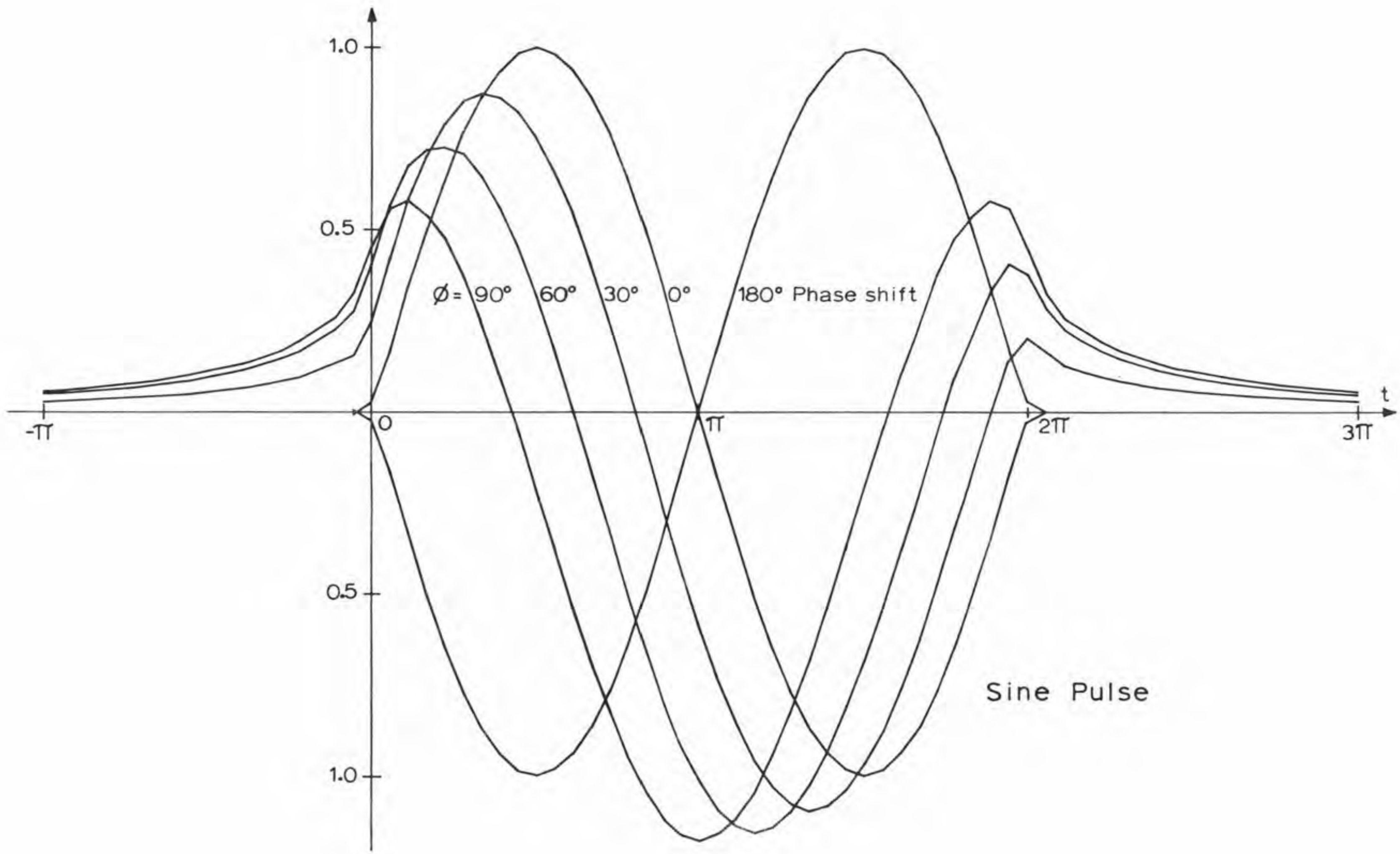

FIG. 1 PULSE DISTORTION DUE TO PHASE SHIFT

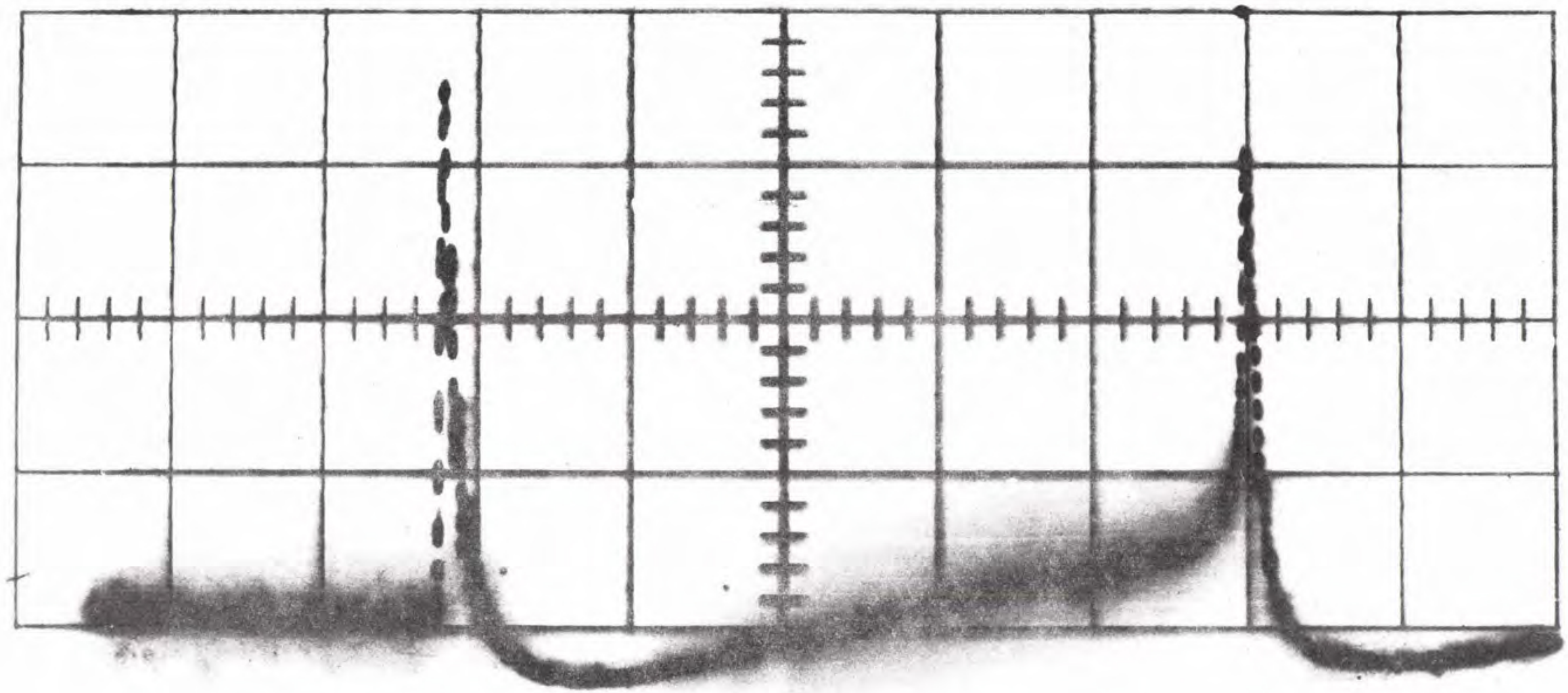

FIG. 2 RECORDING OF SHOCK PULSE AND FIRST BUBBLE PULSE FROM 200 gm TNT BOMBETTA

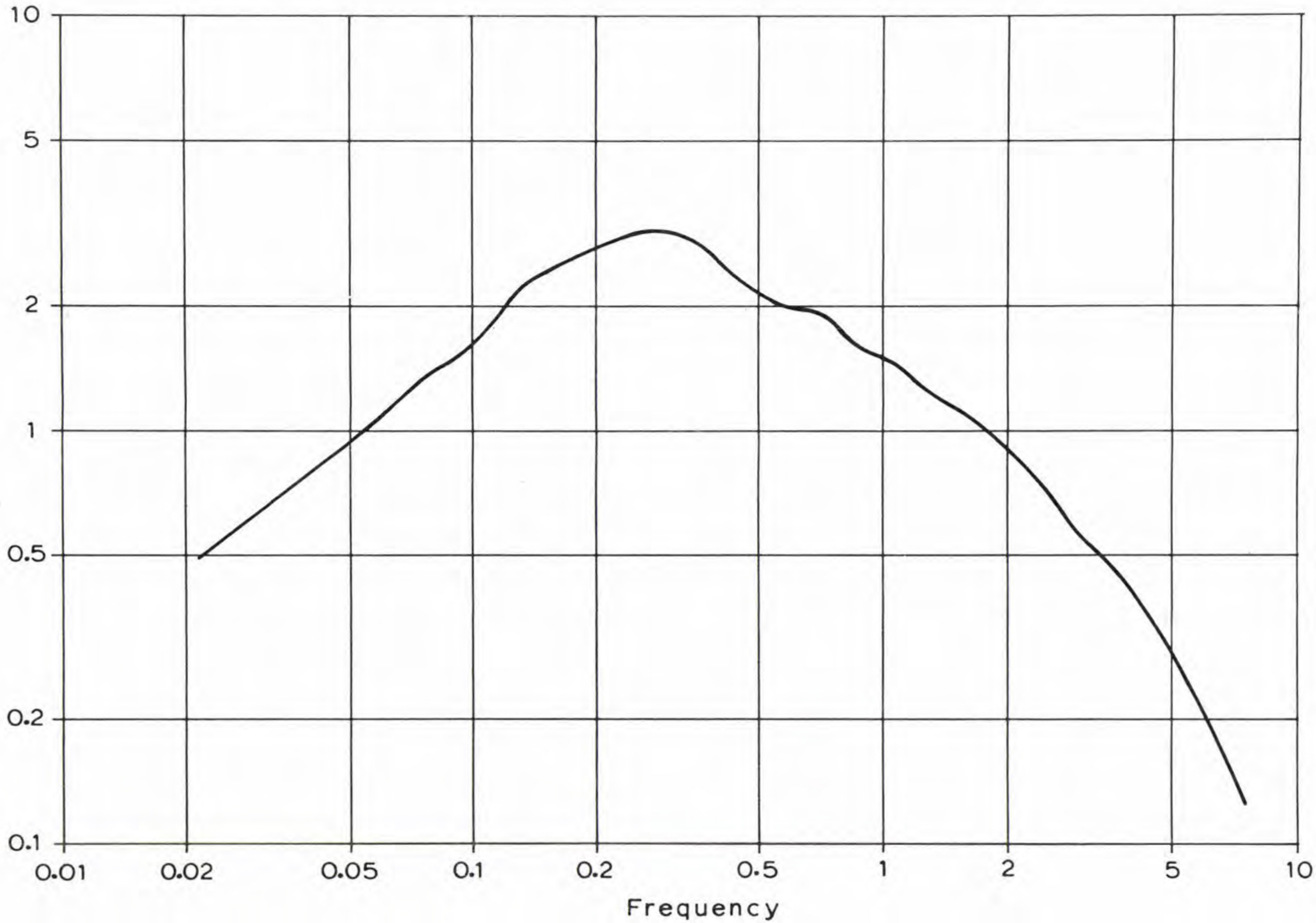

FIG. 3 SPECTRUM OF SHOCK PULSE

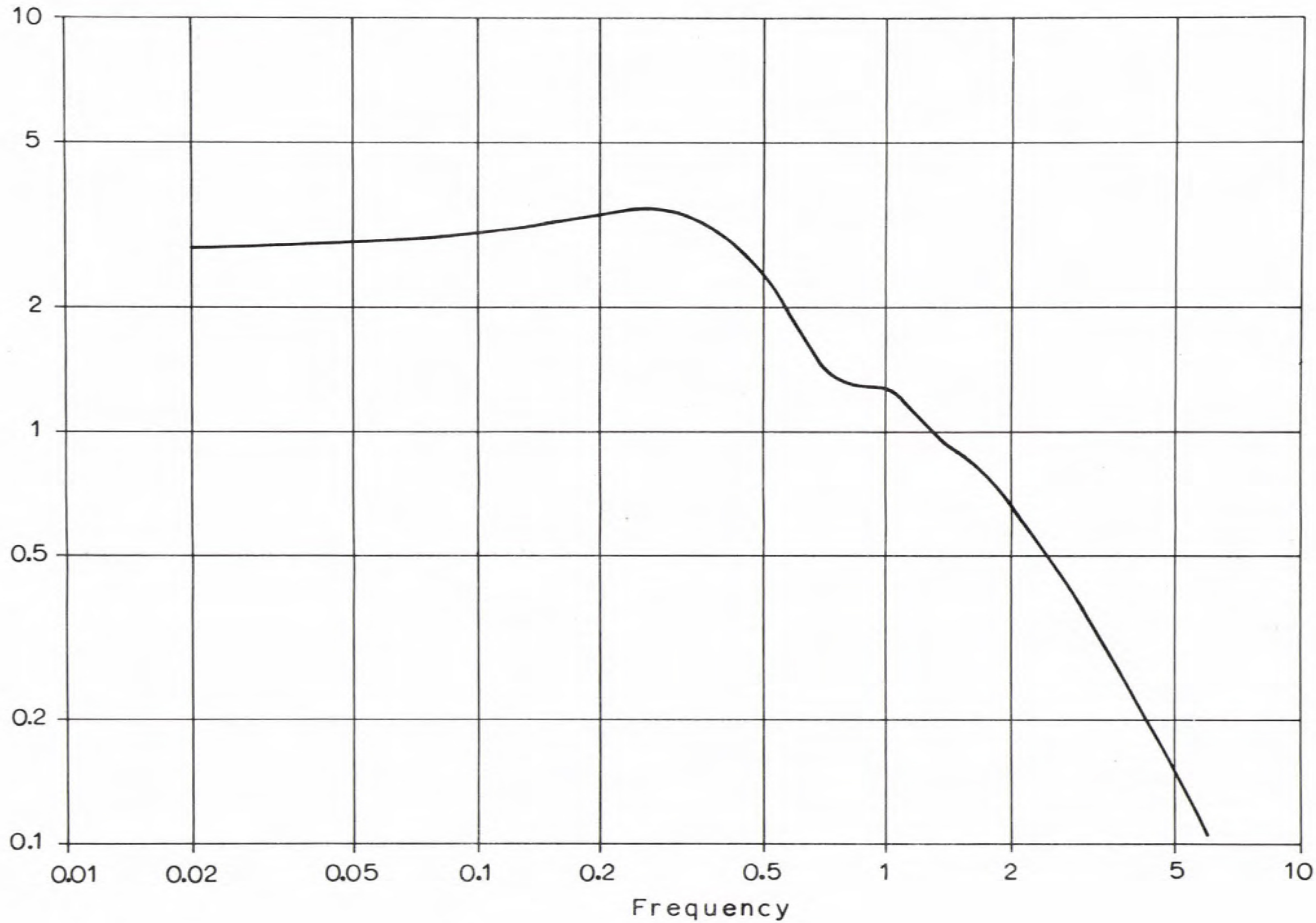

FIG. 4 SPECTRUM OF BUBBLE PULSE

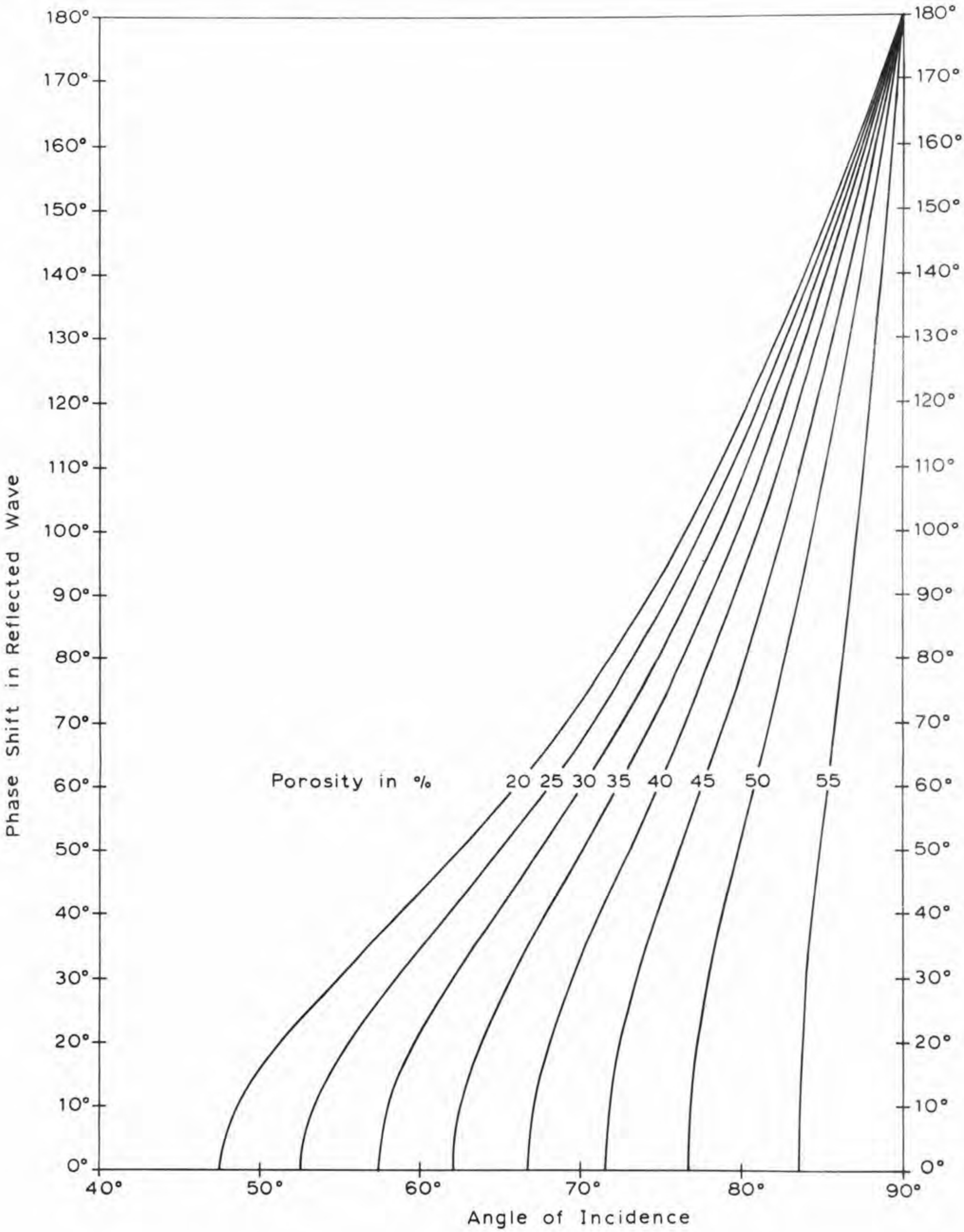

FIG. 5 PHASE SHIFT VS ANGLE OF INCIDENCE AND POROSITY

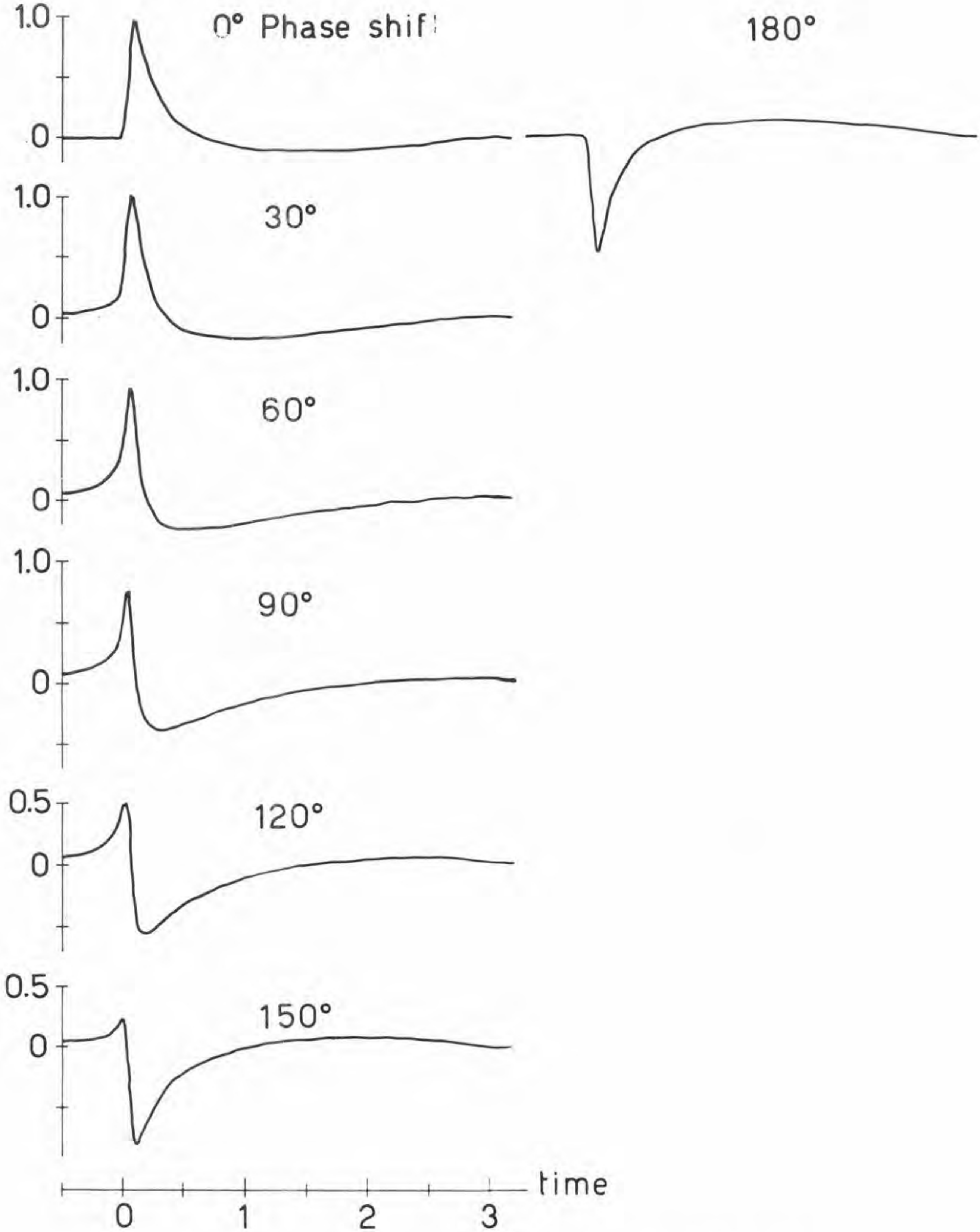

FIG. 6 REFLECTION OF SHOCK PULSE AFTER THE CRITICAL ANGLE

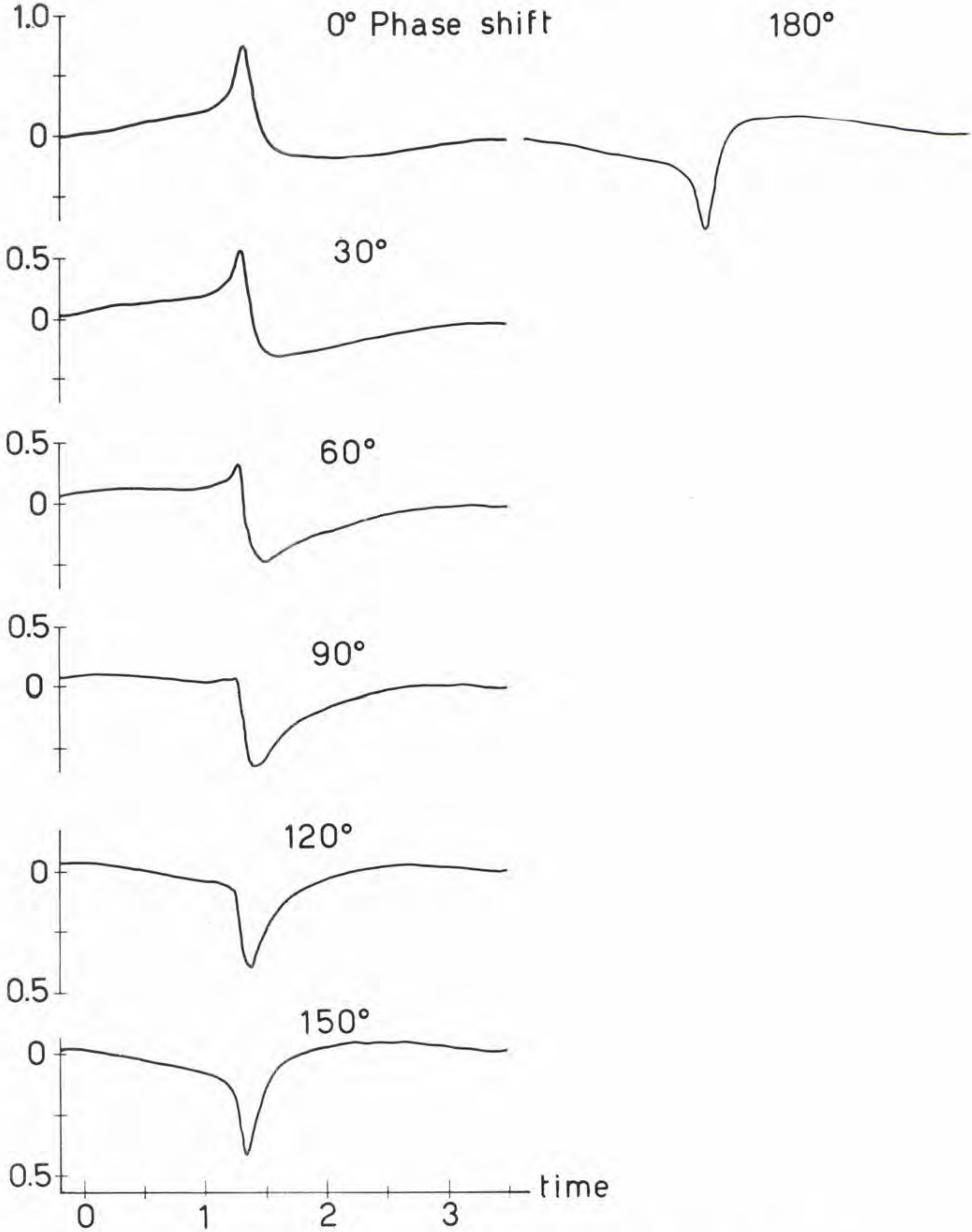

FIG. 7 REFLECTION OF BUBBLE PULSE AFTER THE CRITICAL ANGLE

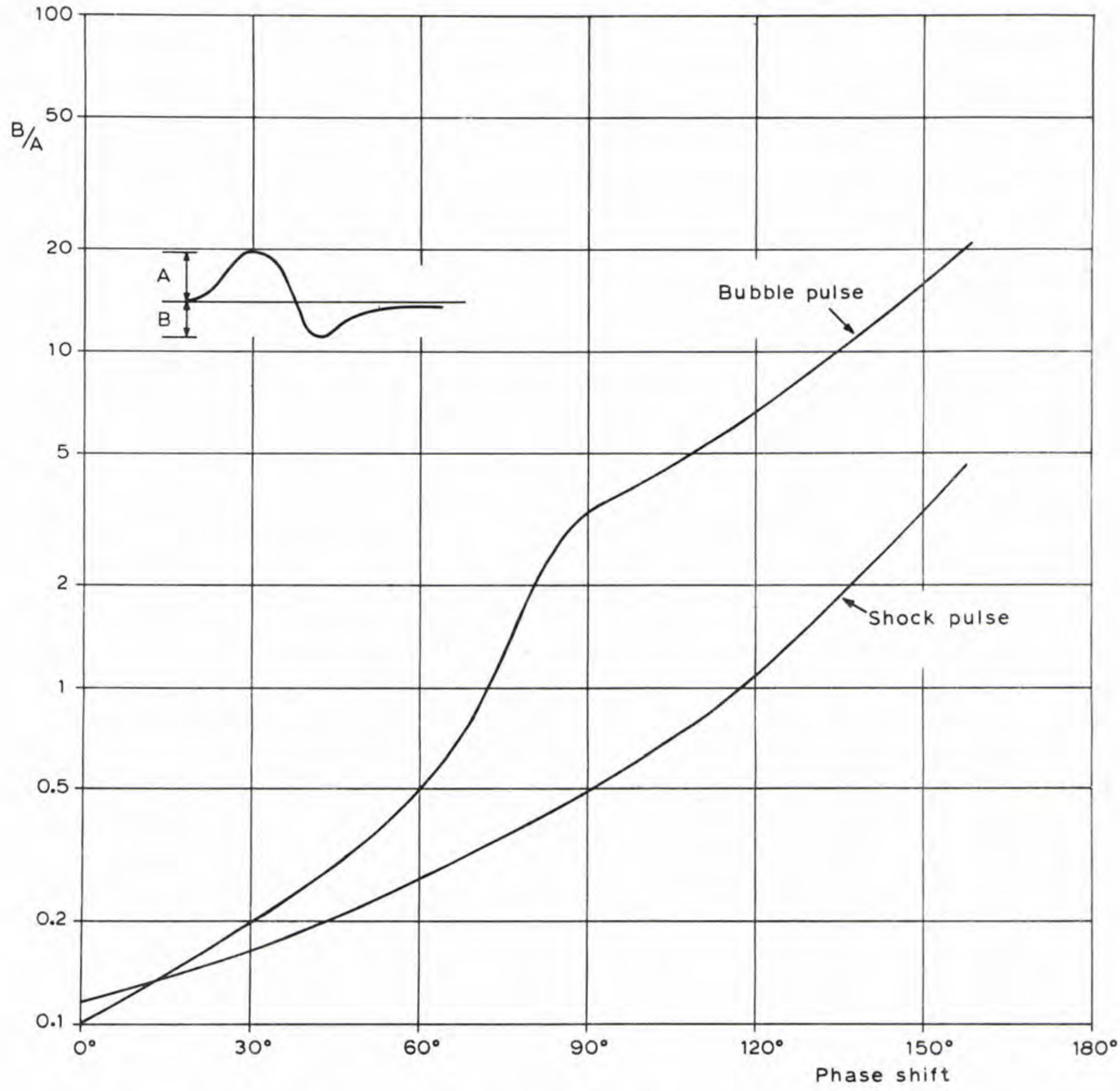

FIG. 8 RATIO BETWEEN FIRST POSITIVE AND NEGATIVE PEAK AMPLITUDES

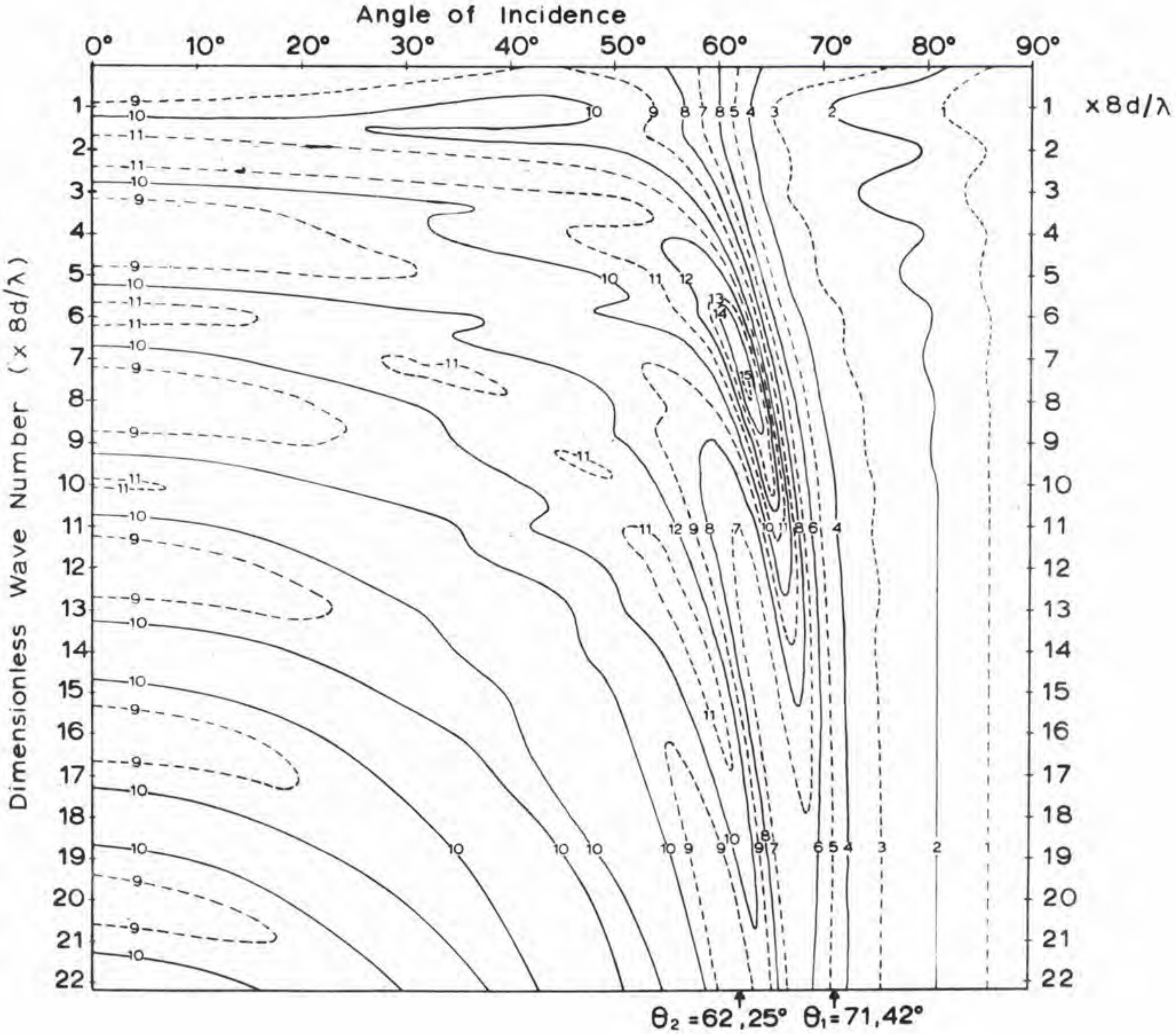

FIG. 9 REFLECTION LOSS IN db AS A FUNCTION OF THE ANGLE OF INCIDENCE AND THE WAVE NUMBER — MODEL A

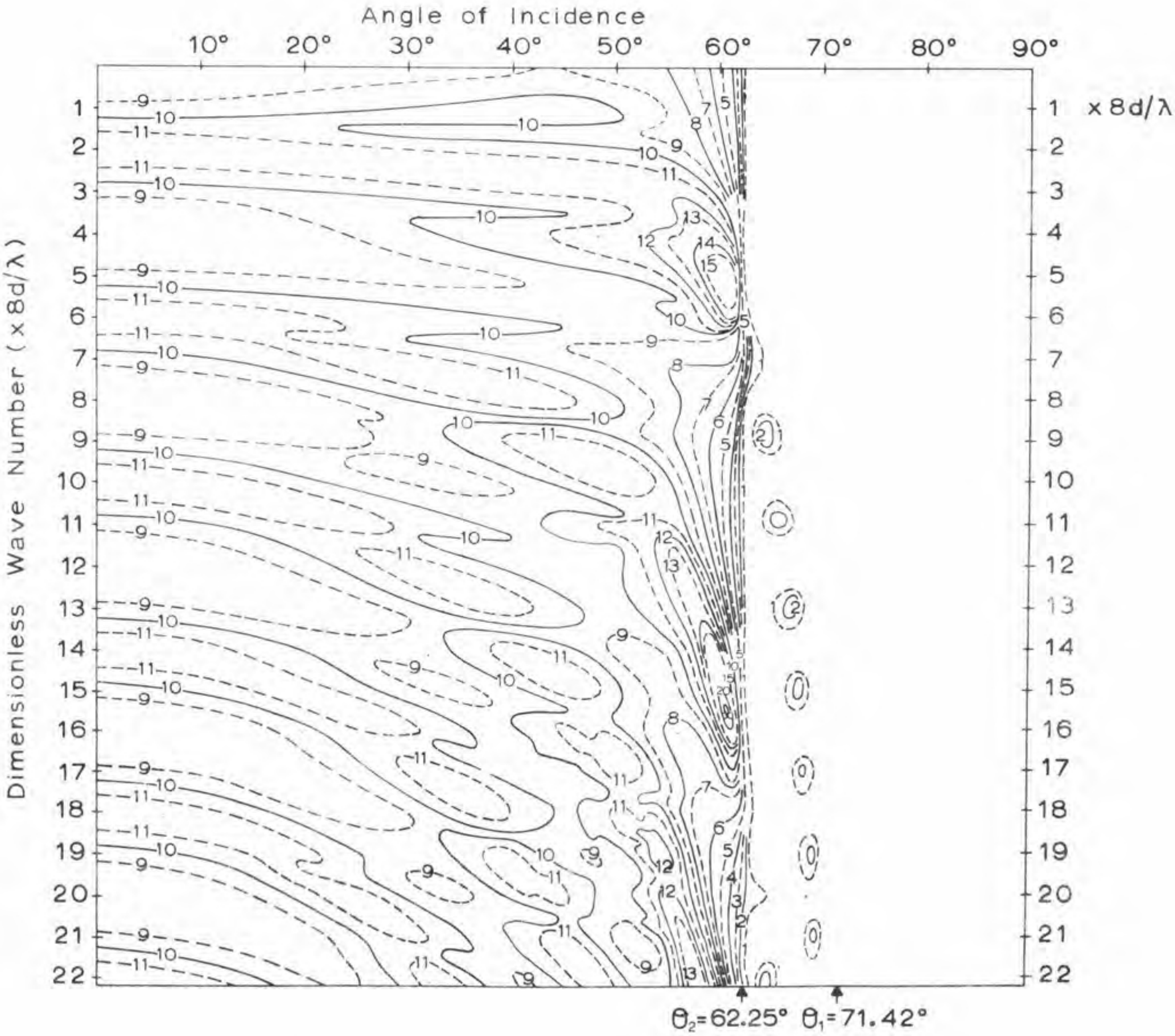

FIG. 10 REFLECTION LOSS IN db AS A FUNCTION OF THE ANGLE OF INCIDENCE AND THE WAVE NUMBER — MODEL A, NO DAMPING

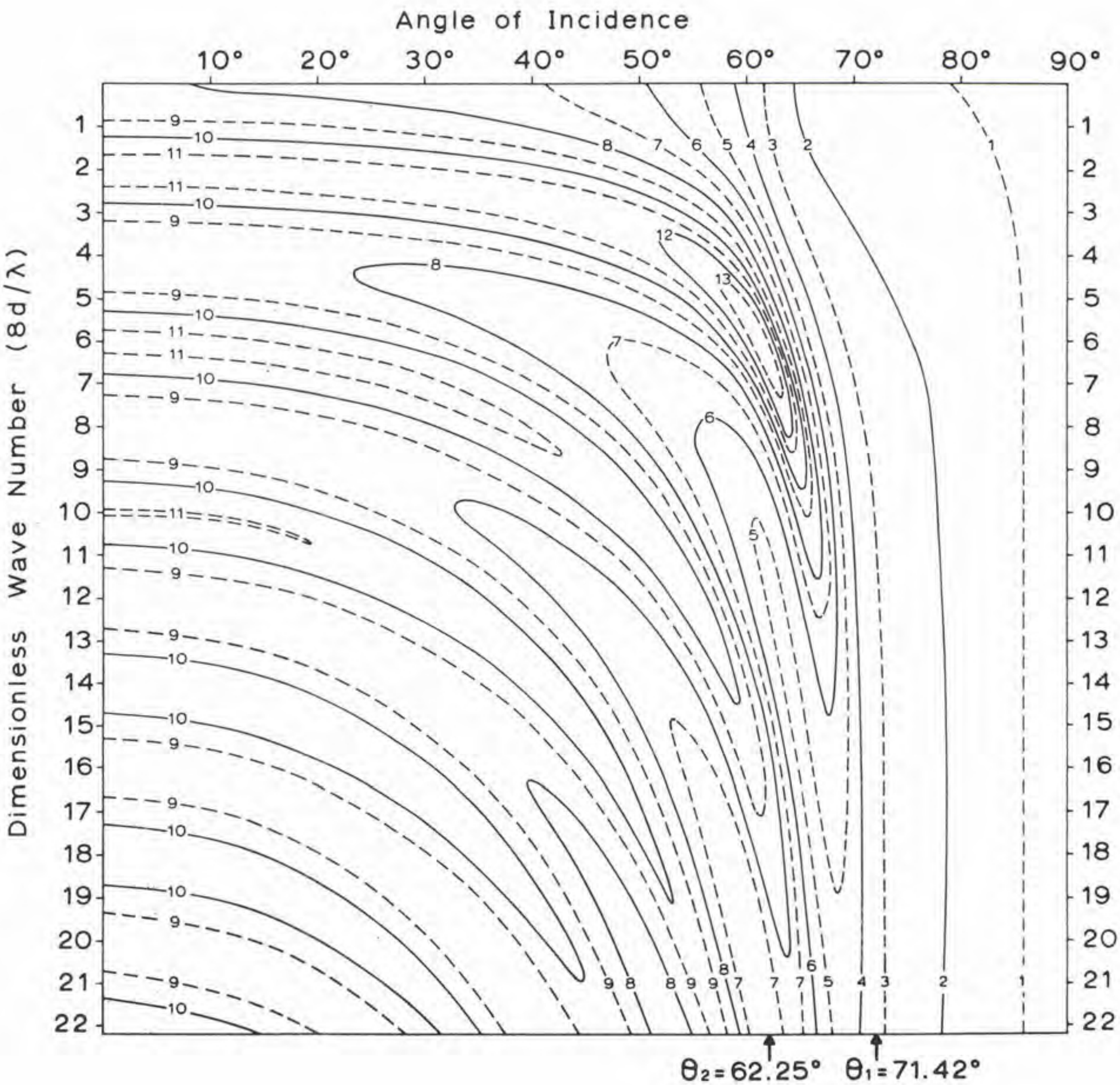

FIG. 11 REFLECTION LOSS IN db AS A FUNCTION OF THE ANGLE OF INCIDENCE AND THE WAVE NUMBER — MODEL A, NO SHEAR

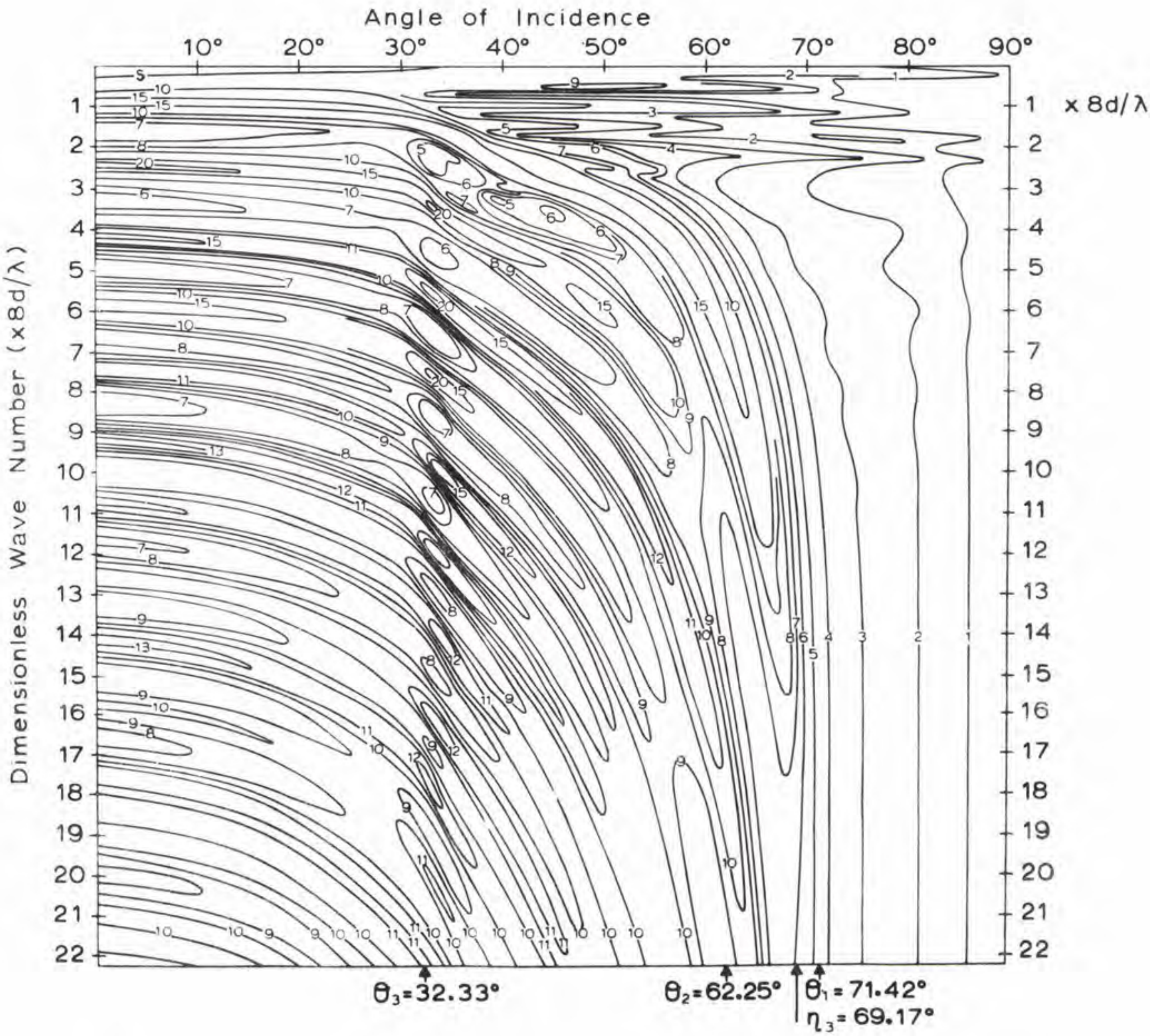

FIG. 12 REFLECTION LOSS IN db AS A FUNCTION OF THE ANGLE OF INCIDENCE AND THE WAVE NUMBER — MODEL B

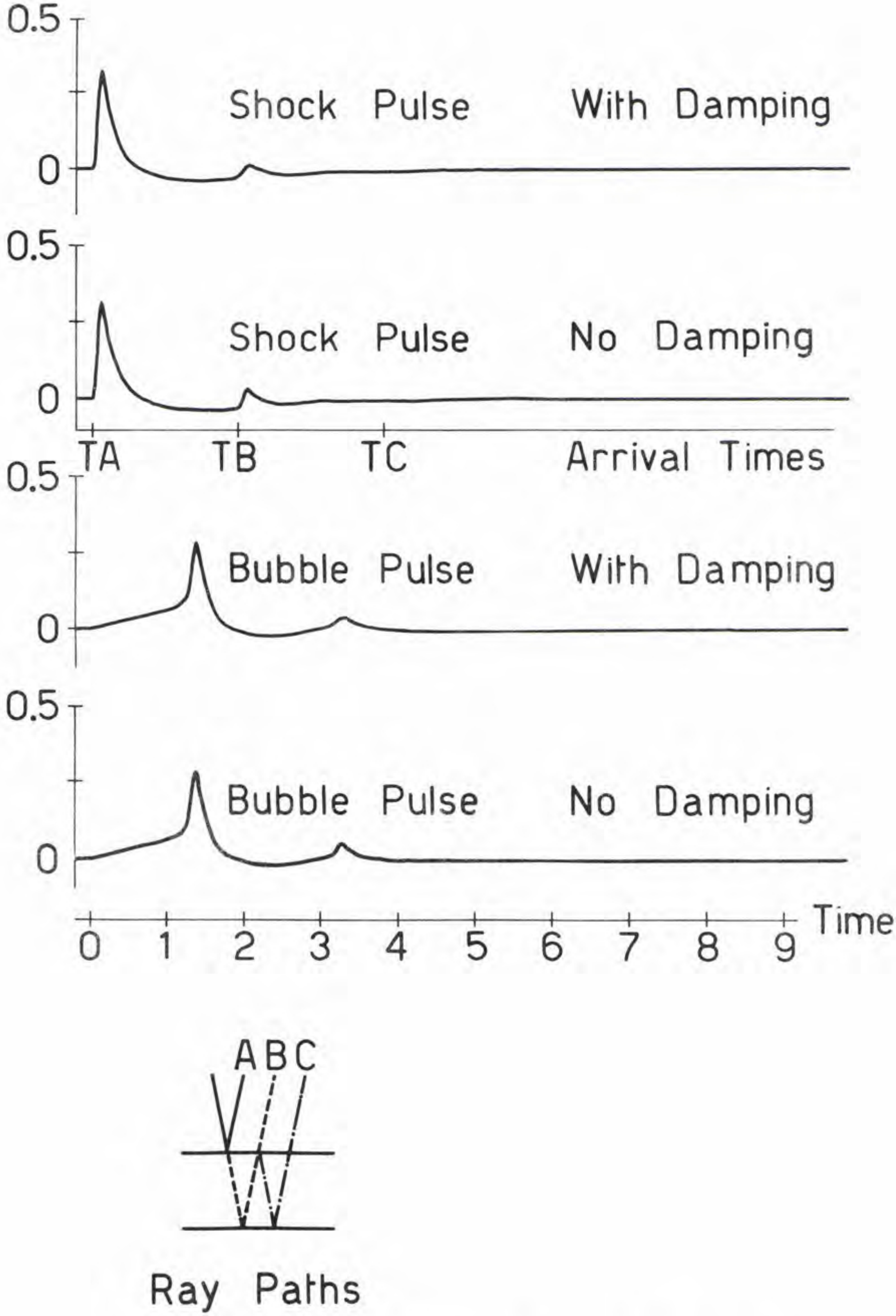

FIG. 13 PULSE SHAPE FROM VERTICAL INCIDENCE – MODEL A

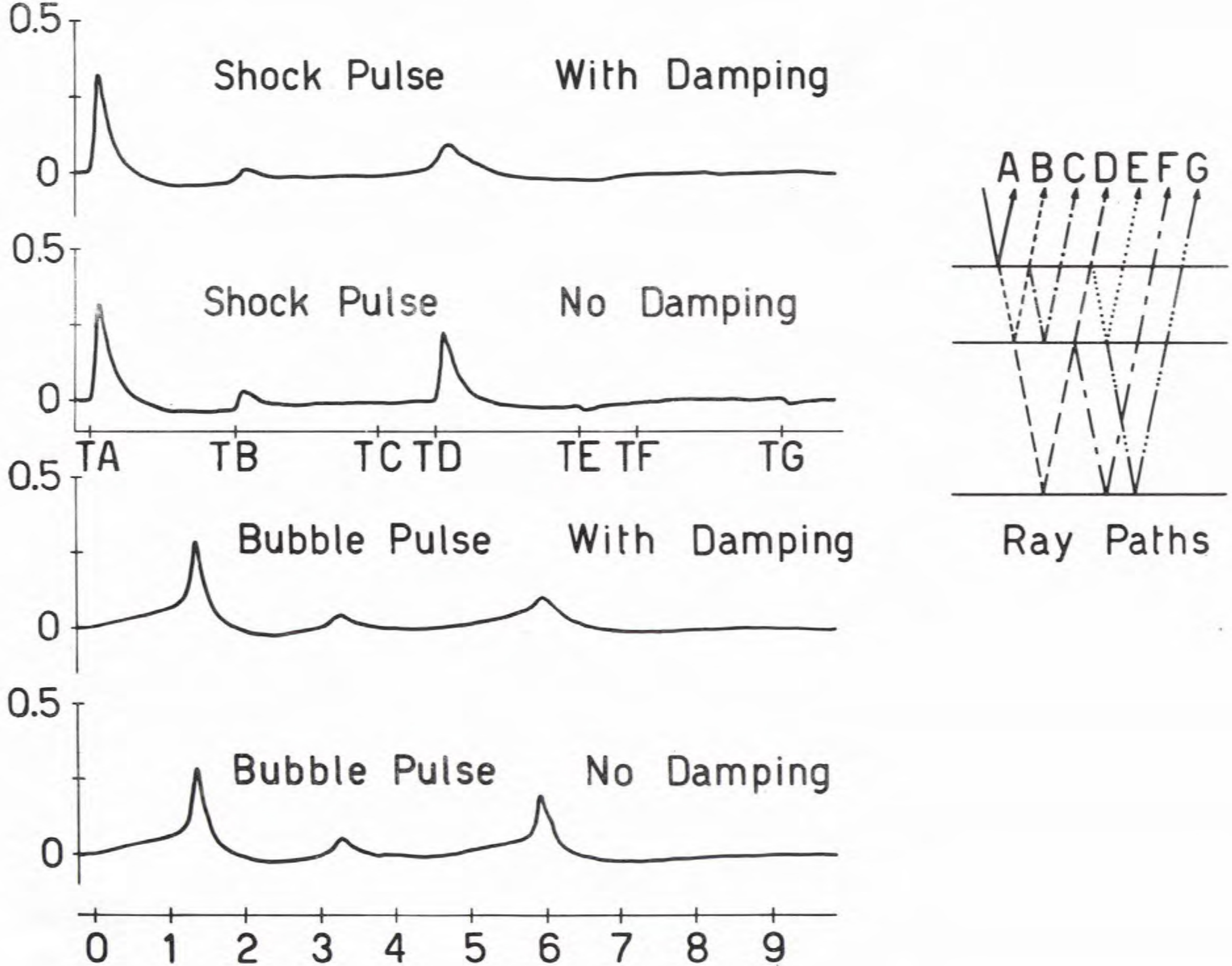

FIG. 14 PULSE SHAPE FROM VERTICAL INCIDENCE – MODEL B

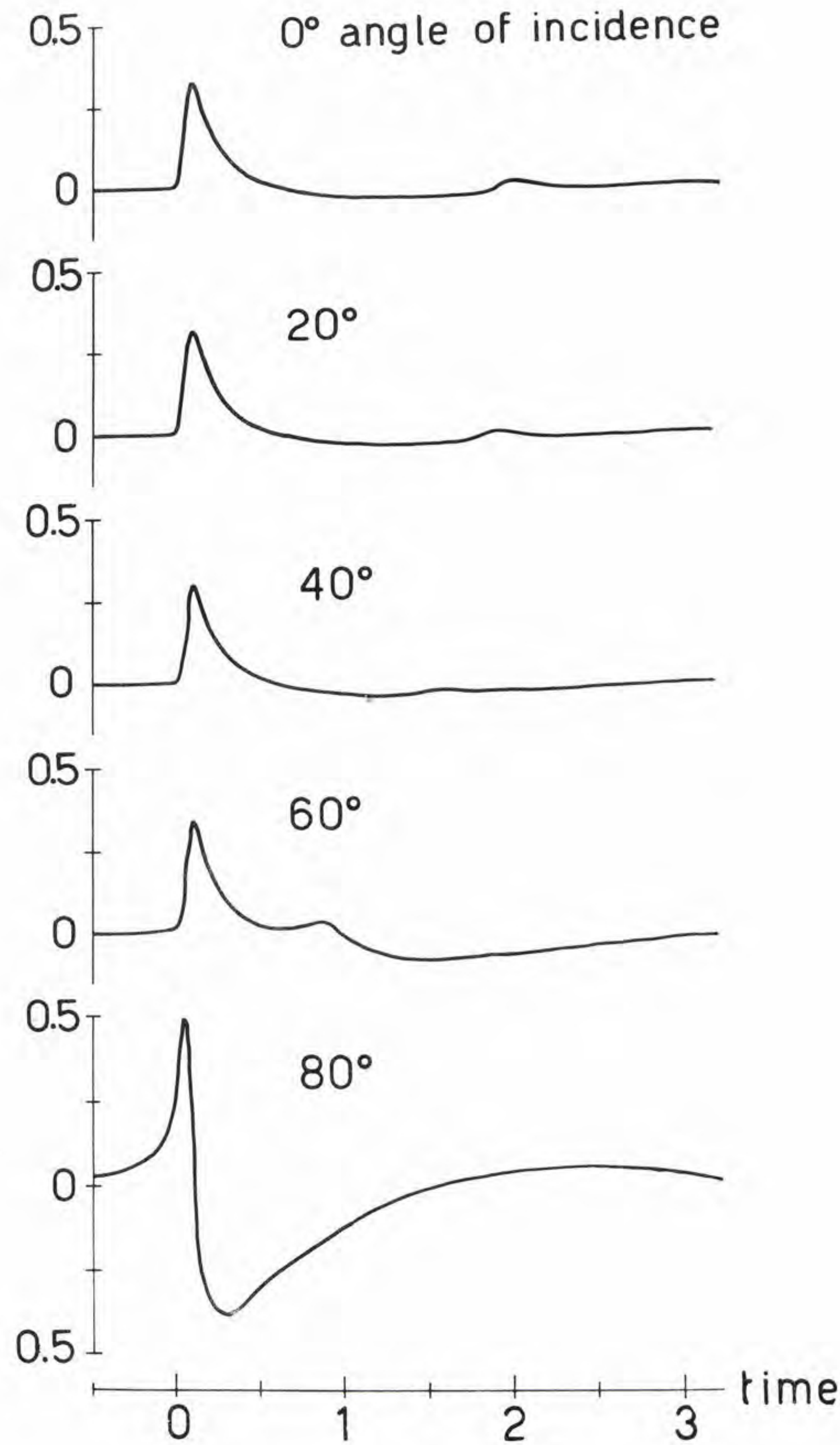

FIG. 15 REFLECTION OF SHOCK PULSE – MODEL A

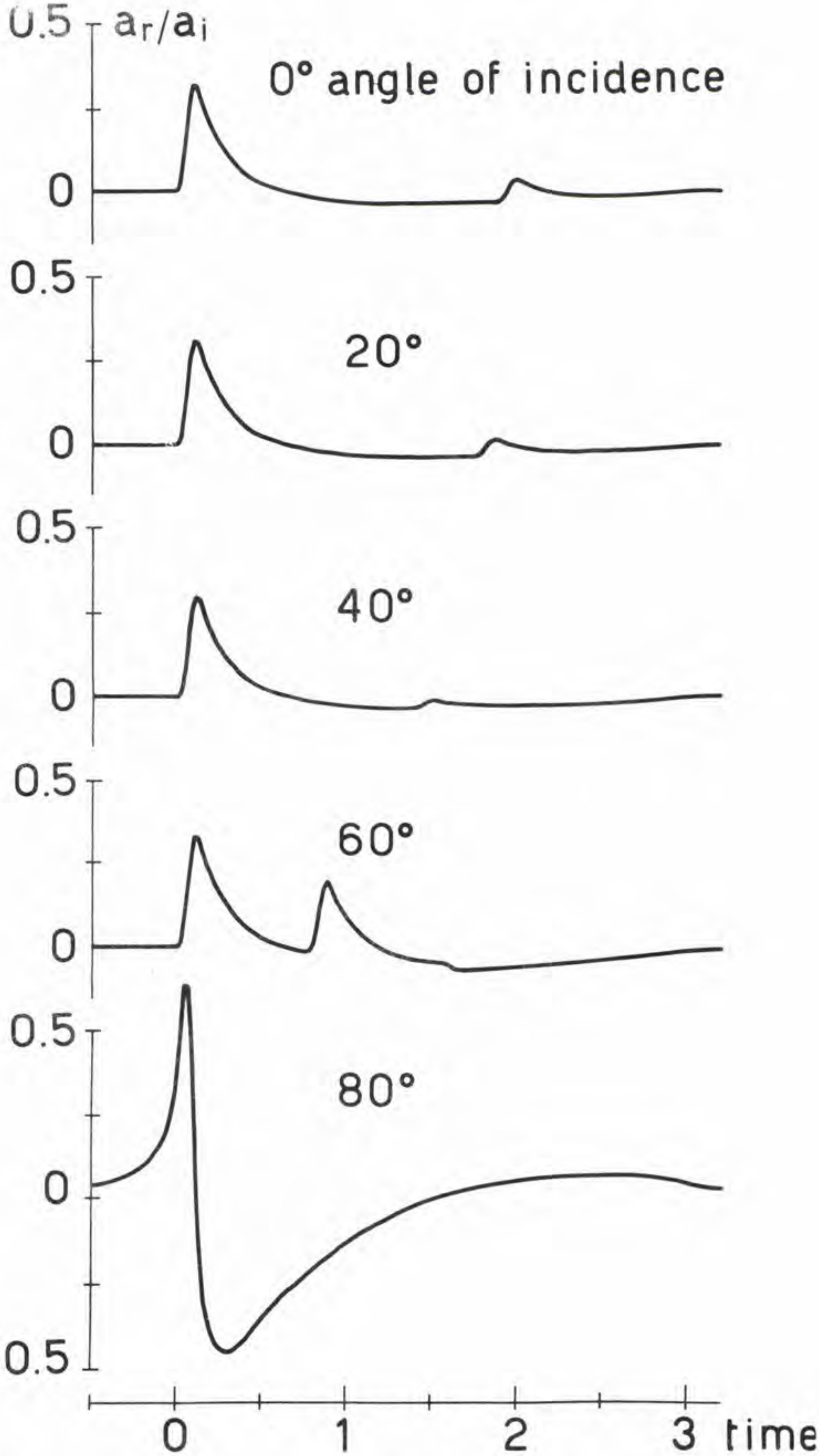

FIG. 16 REFLECTION OF SHOCK PULSE – MODEL A, NO DAMPING

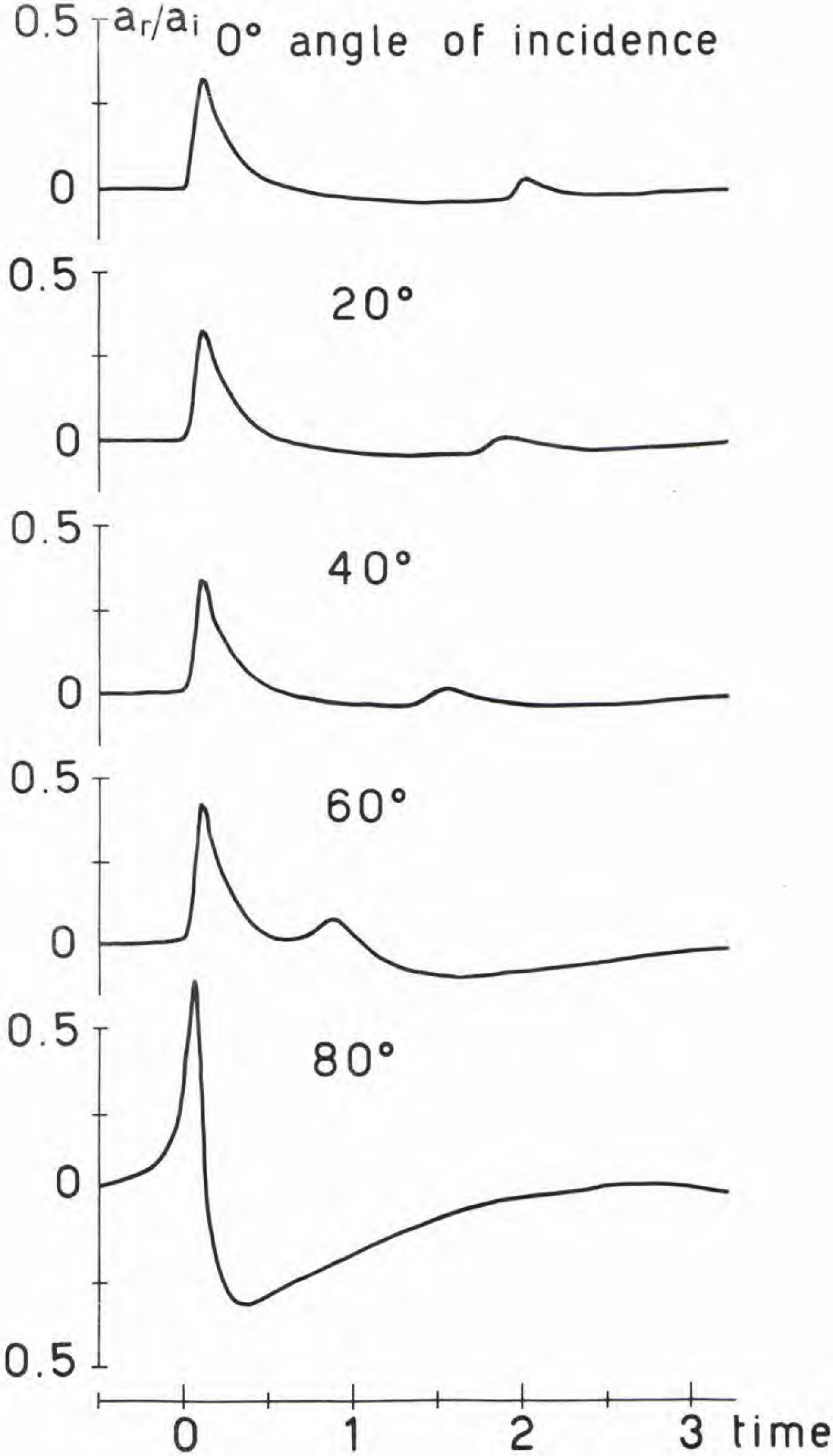

FIG. 17 REFLECTION OF SHOCK PULSE – MODEL A, NO SHEAR

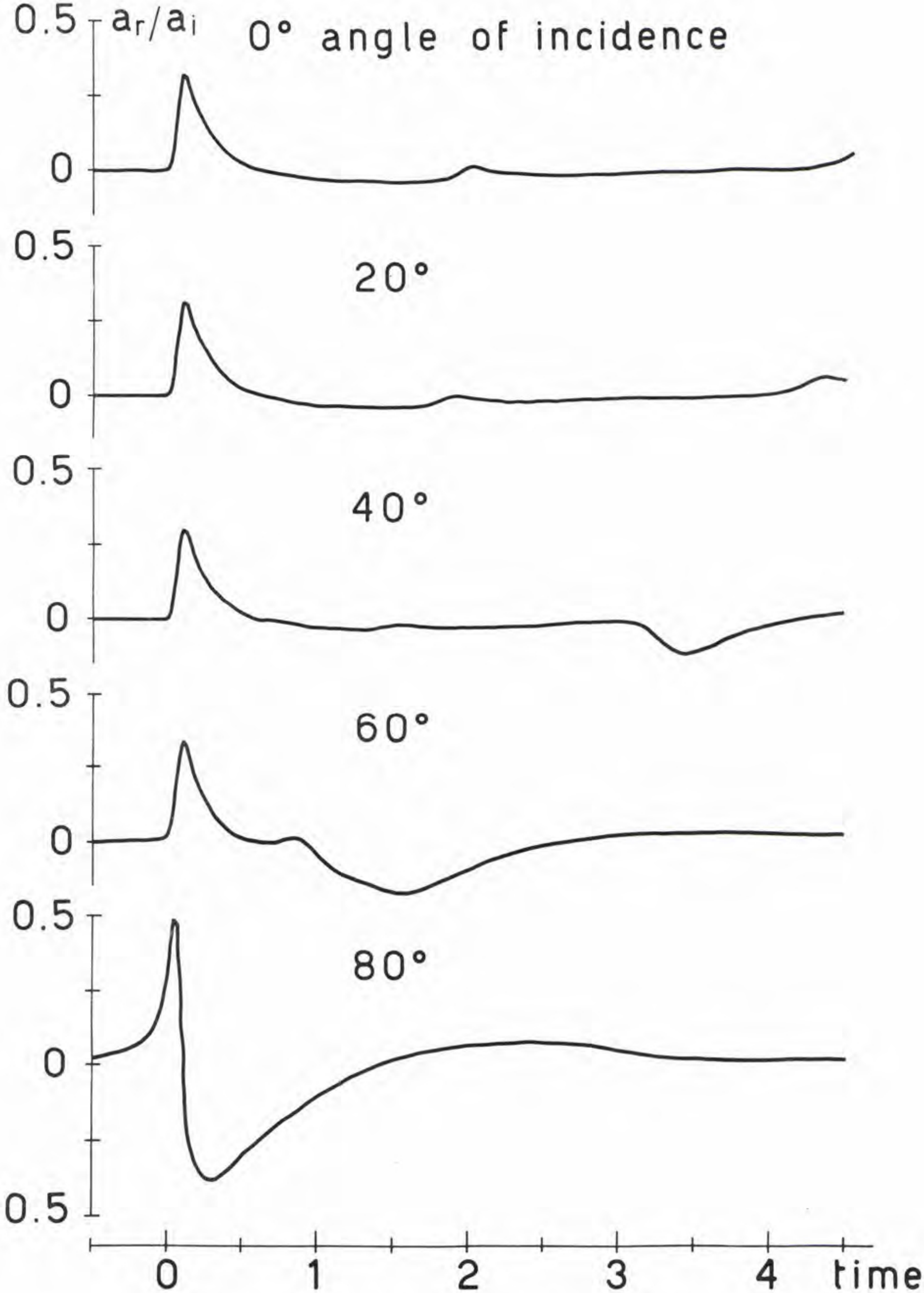

FIG. 18 REFLECTION OF SHOCK PULSE – MODEL B

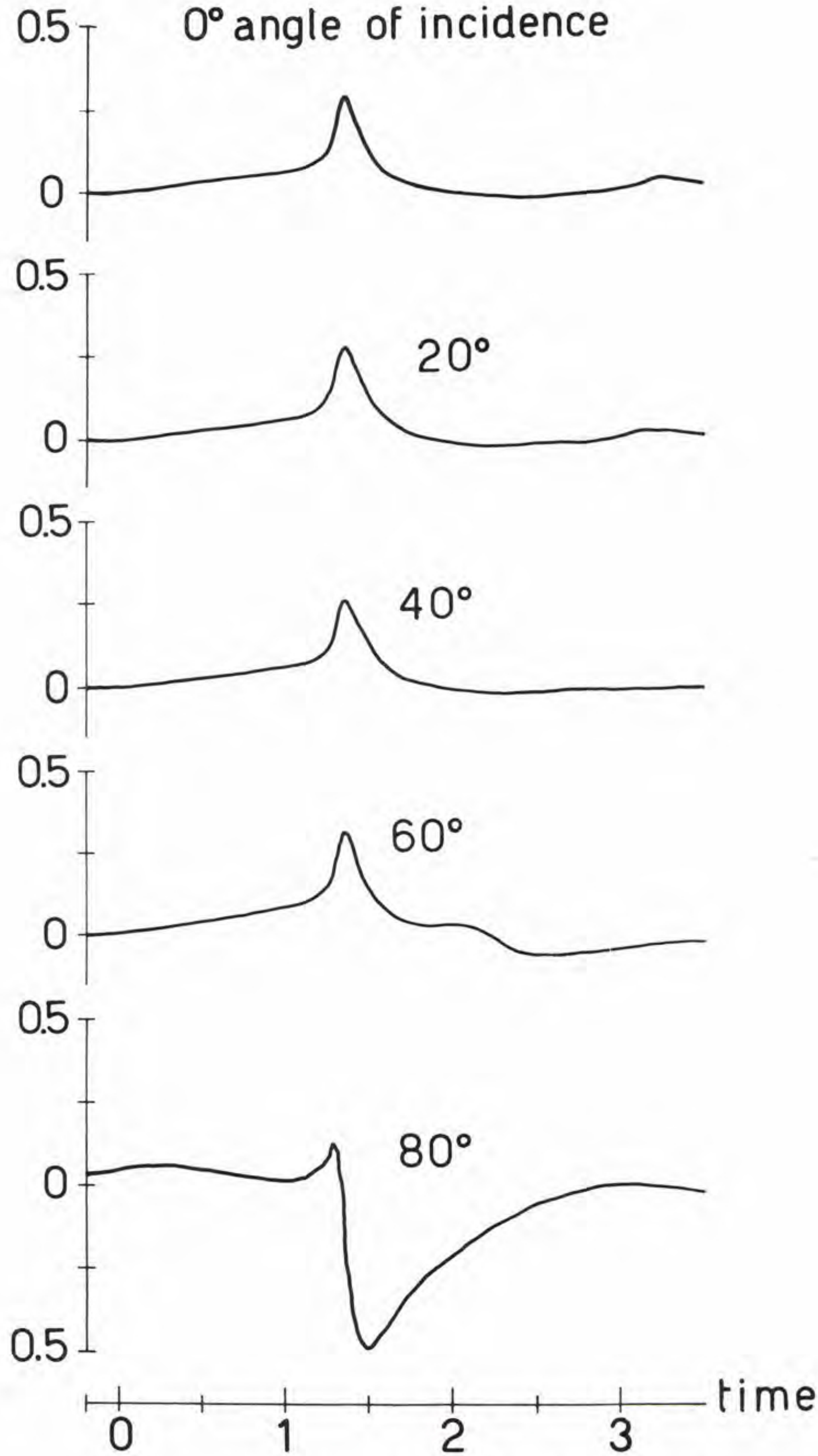

FIG. 19 REFLECTION OF BUBBLE PULSE – MODEL A

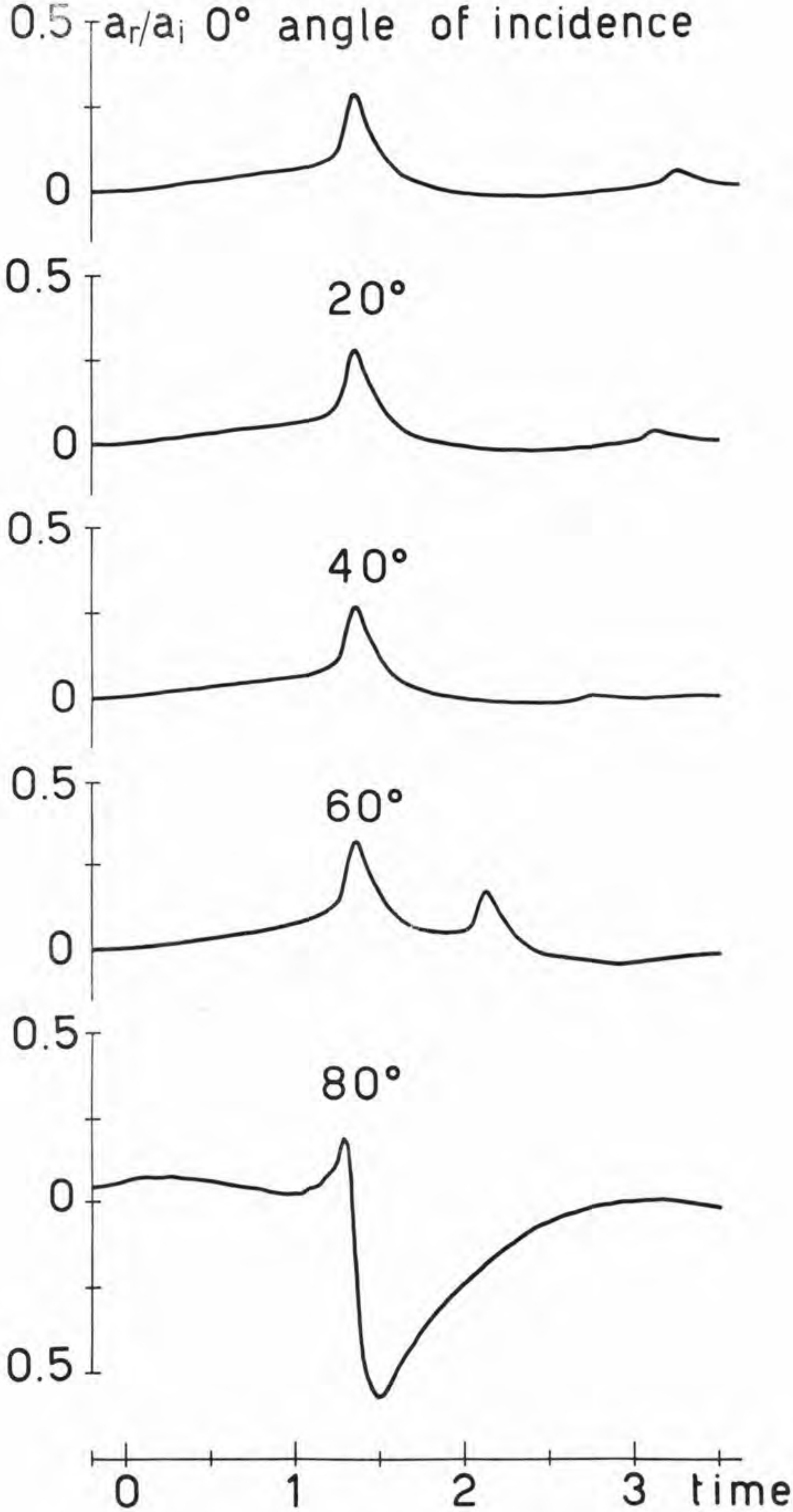

FIG. 20 REFLECTION OF BUBBLE PULSE – MODEL A, NO DAMPING

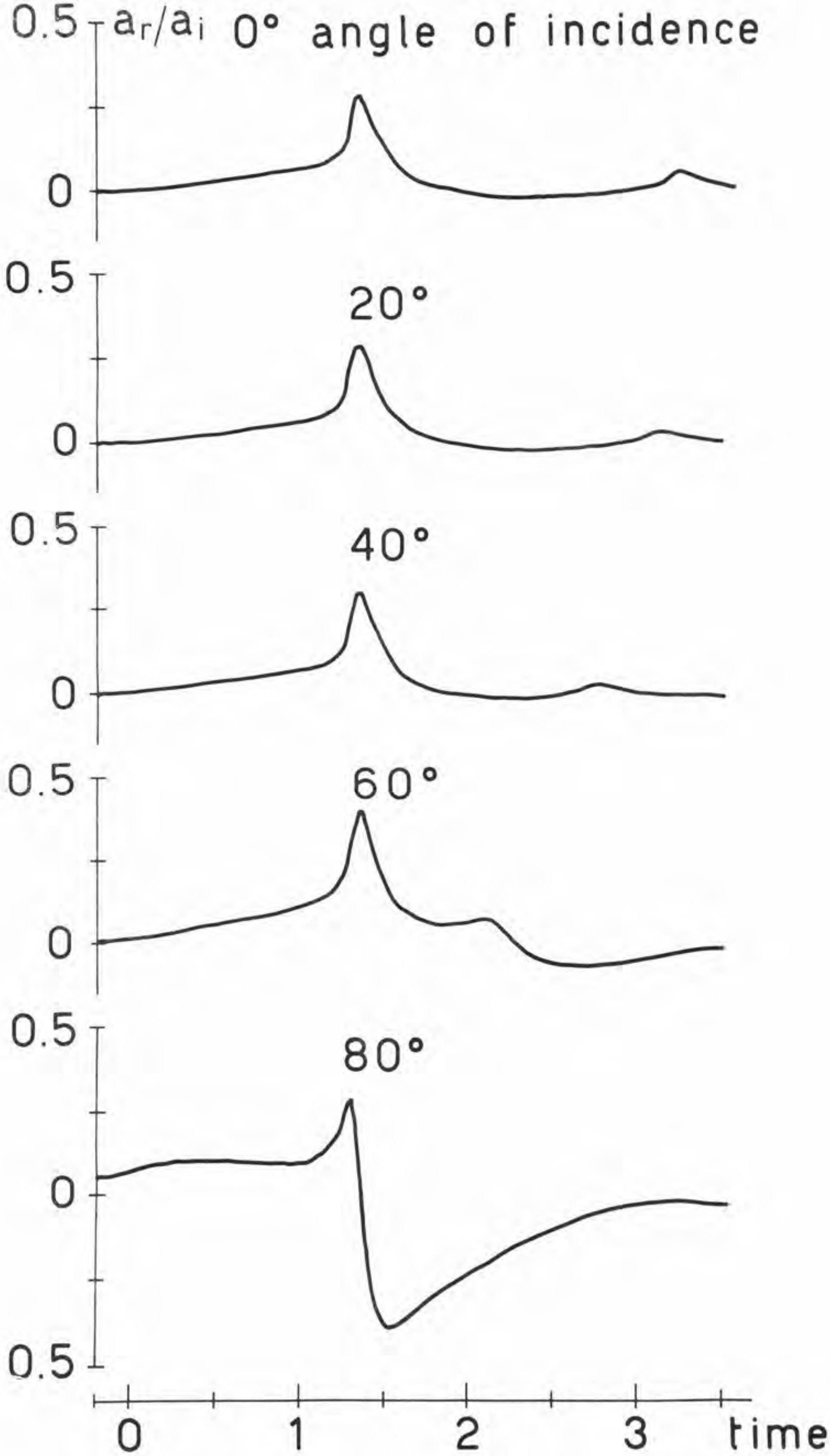

FIG. 21 REFLECTION OF BUBBLE PULSE – MODEL A, NO SHEAR

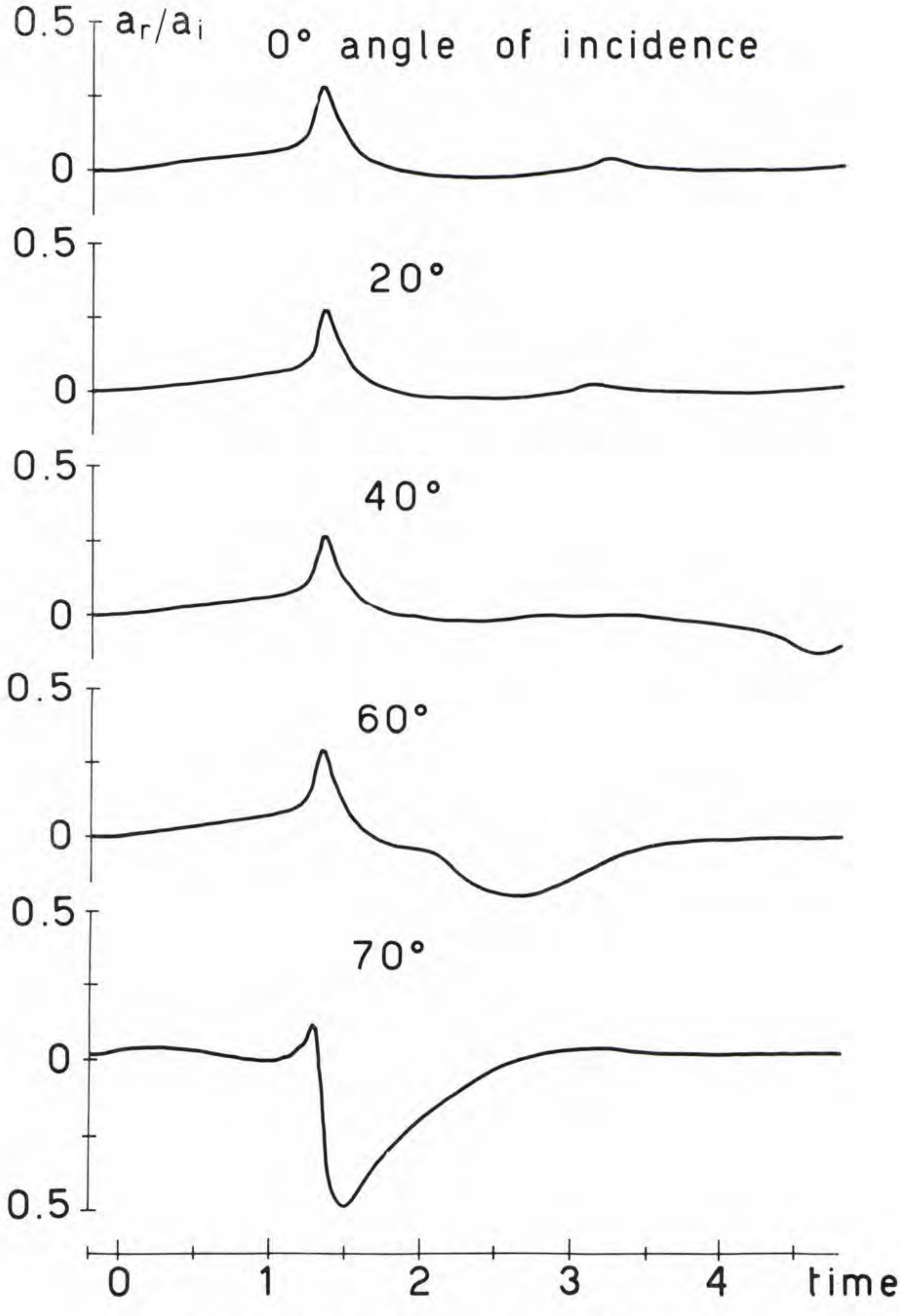

FIG. 22 REFLECTION OF BUBBLE PULSE – MODEL B

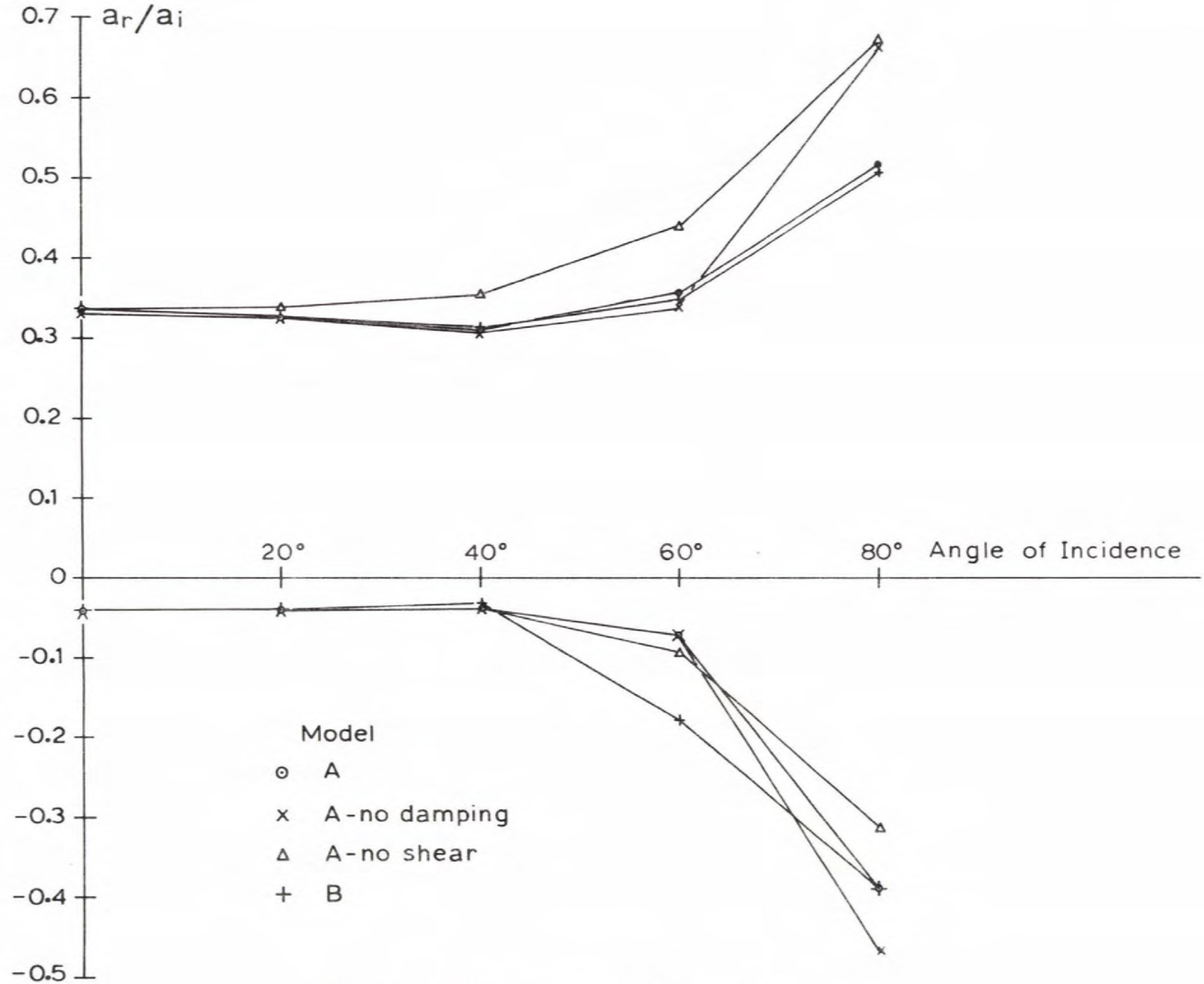

FIG. 23 AMPLITUDES OF REFLECTED SHOCK PULSE

DISTRIBUTION LIST

MINISTRIES OF DEFENCE

Minister of Defence Brussels, Belgium	10 copies
Department of National Defence Ottawa, Canada	10 copies
Chief of Defence Copenhagen, Denmark	10 copies
Minister of National Defence Paris, France	10 copies
Minister of Defence Federal Republic of Germany Bonn, Germany	12 copies
Minister of Defence Athens, Greece	10 copies
Minister of National Defence Rome, Italy	10 copies
Minister of National Defence The Hague, Netherlands	10 copies
Minister of National Defence Oslo, Norway	10 copies
Minister of National Defence Lisbon, Portugal	10 copies
Minister of National Defence Ankara, Turkey	10 copies
Minister of Defence London, England, U.K.	20 copies
SECDEF United States (through USNLO to SACLANTCEN, ONR, London)	70 copies

NATO AUTHORITIES

Standing Group NATO Washington D.C. 20301	3 copies
SECGEN NATO (through SGREP) Paris, France	5 copies
ASG for Scientific Affairs NATO Paris, France	1 copy
SACLANT Norfolk, Virginia 23511	3 copies
SACEUR Paris, France	7 copies
CINCHAN Ft. Southwick, Fareham England	1 copy
SACLANTREPEUR Paris, France	1 copy
COMAIRCHAN Northwood, England	1 copy
CINCAFMED Malta G.C.	1 copy
CINCEASTLANT Eastbury Park Northwood, England	1 copy
CINCWESTLANT Norfolk, Virginia 23511	1 copy
COMMAIREASTLANT Northwood, England	1 copy
COMSUBEASTLANT Ft. Blockhouse Gosport, England	1 copy
COMCANLANT H.M.C. Dockyard Halifax, Canada	1 copy
COMOCEANLANT Norfolk, Virginia 23511	1 copy
COMEDCENT Naples, Italy	1 copy
COMEDSOUEAST Malta G.C.	1 copy
COMSUBACLANT Norfolk, Virginia 23511	1 copy
COMSUBMED Malta G.C.	1 copy
Commander TASK FORCE 442 FPO, N.Y. 09521	1 copy
SHAPE T.C. The Hague, Netherlands	1 copy

SCIENTIFIC COMMITTEE OF NATIONAL REPRESENTATIVES FOR SACLANTCEN

SCNR Belgium	1 copy
SCNR Canada	1 copy
SCNR Denmark	1 copy
SCNR France	1 copy
SCNR Germany	1 copy
SCNR Greece	1 copy
SCNR Italy	1 copy
SCNR Netherlands	1 copy
SCNR Norway	1 copy
SCNR Turkey	1 copy
SCNR United Kingdom	1 copy
SCNR United States	1 copy

NATIONAL LIAISON OFFICERS FOR SACLANTCEN

NLO France	1 copy
NLO Italy	1 copy
NLO Portugal	1 copy
NLO United States	1 copy

NATIONAL LIAISON REPRESENTATIVES TO SACLANT

NLR Belgium	1 copy
NLR Canada	1 copy
NLR Denmark	1 copy
NLR France	1 copy
NLR Germany	1 copy
NLR Greece	1 copy
NLR Italy	1 copy
NLR Netherlands	1 copy
NLR Norway	1 copy
NLR Portugal	1 copy
NLR Turkey	1 copy
NLR United Kingdom	1 copy